ELSEVIER

Tectonophysics 268 (1996) 65–81

TECTONOPHYSICS

Magmatism and the geodynamics of rifting of the Pripyat–Dnieper–Donets rift, East European Platform

Marjorie Wilson [a,*], Zoya M. Lyashkevich [b]

[a] *Department of Earth Sciences, Leeds University, Leeds LS2 9JT, UK*
[b] *Institute of Fossil Fuels and Endogenous Processes, National Academy of Sciences of Ukraine, Lvov, Ukraine*

Received 31 January 1996; accepted 31 May 1996

Abstract

The distribution of volcanism in the Late Devonian Pripyat–Dnieper–Donets rift within the East European Platform, based upon the results of deep drilling, indicates that pre-existing basement structures and the major rift-bounding faults played an important role in channelling the magmas towards the surface. Major- and trace-element and Sr–Nd isotopic studies of the most primitive basic and ultrabasic magmas, combined with estimates of the amount of extension ($\beta = 1.1$ to 1.3), strongly suggest that magmatism was triggered by the upwelling of a thermally and geochemically anomalous mantle plume from the deep mantle during the Late Frasnian. The peak of the magmatism occurred in the Famennian, coincident with the maximum amount of lithospheric extension. Magmatism, rifting and domal basement uplift were contemporaneous at several localities within the EEP, suggesting that the thermal and geodynamic evolution of the platform could have been influenced by a cluster of mantle plumes during the Late Devonian.

Keywords: Pripyat–Dnieper–Donets rift; magmatism; Devonian; East European Platform; plumes

1. Introduction

The East European Platform (EEP) extends from the Tornquist–Teisseyre Zone to the Urals and from the Barents Sea to the Peri-Caspian Basin. Once considered as one of the most stable blocks of the Earth's crust, its sedimentary record shows that after its consolidation in the Proterozoic it was repeatedly affected by rifting cycles that were separated by periods of tectonic quiescence and phases of intraplate compression (Nikishin et al., 1996). During the Late Devonian, rifting, locally associated with domal basement uplift and magmatism, was widespread from the Pripyat–Dnieper–Donets (PDD) rift in the south to the Eastern Barents Sea in the north (Fig. 1).

The Late Devonian magmatism of the Kola Peninsula and adjacent Archangelsk region constitutes one of the world's largest alkaline igneous provinces, comprising 25 magmatic centres within an area of 100,000 km^2. Magmatic activity occurred between 380 and 360 Ma and coincided with the subsidence of the NE–SW-trending Kontozero graben (Kramm et al., 1993). There have been several recent geochemical and Sr–Nd isotope studies of the Kola Alkaline Province (e.g., Kramm et al., 1993; Kramm and Kogarko, 1994; Zaitsev and Bell, 1995). In contrast, the magmatism of the Pripyat–Dnieper–Donets rift in the south of the platform has received little at-

* Corresponding author. FAX: +44.113.233-6619.

PII S0040-1951(96)00234-X

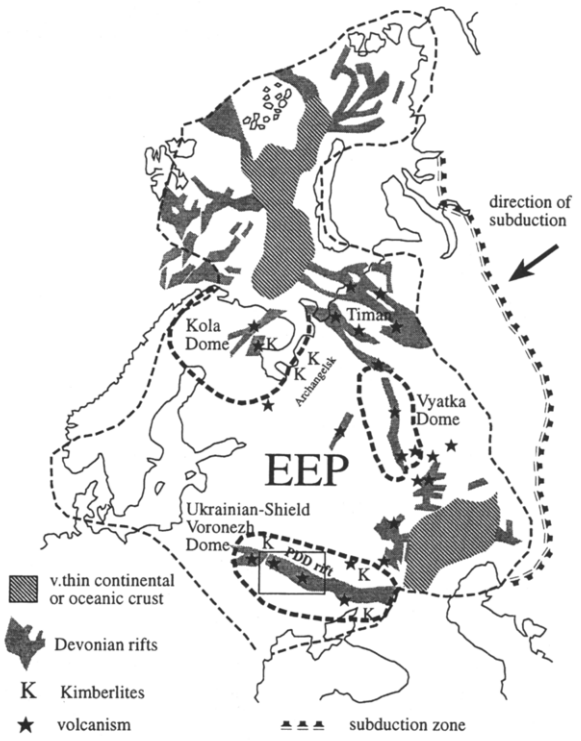

Fig. 1. Map of the East European Platform showing the location of the main areas of Late Devonian rifting and associated volcanism. Rectangle indicates the area of the Pripyat–Dnieper–Donets rift. After Nikishin et al. (1996).

tention in western literature, apart from brief descriptions by Chekunov et al. (1992) and Wilson (1993a).

Alkaline–ultrabasic magmatism with kimberlite affinities appears to have occurred at widely scattered localities across the EEP during the Late Devonian (Gon'shakova et al., 1967; Mahotkin and Juravlev, 1993; de Boorder et al., 1996; Fig. 1), often associated with more extensive Frasnian–Famennian volcanism. In addition to the PDD rift, these include a zone between the Donbass segment of the rift and the Sea of Azov, the northeastern flank of the Pripyat Trough, the southeastern flank of the Voronezh Massif, the Kola Peninsula–Archangelsk region and possibly the Timan–Pechora Basin.

This study focuses on the distribution and geochemical characteristics of the magmatism associated with the formation of the Late Devonian Pripyat–Dnieper–Donets rift. Maps constructed on the basis of borehole data clearly indicate the important role that pre-existing basement structures and the major rift-bounding faults played in channelling the magmas towards the surface. Major and trace element and Sr–Nd isotopic studies of the most primitive basic and ultrabasic magmas, combined with estimates of the amount of extension, strongly suggest that magmatism was triggered by the upwelling of a thermally and geochemically anomalous mantle plume from the deep mantle during the Late Frasnian. The peak of the magmatic activity occurred in the Famennian, coincident with the maximum amount of lithospheric extension. Magmatism, rifting and domal basement uplift were contemporaneous at several localities within the EEP, suggesting that the thermal and geodynamic evolution of the platform may have been influenced by a cluster of mantle plumes during the Late Devonian.

2. Pripyat–Dnieper–Donets rift

The NW–SE-trending, 2000-km-long, Pripyat–Dnieper–Donets (PDD) palaeorift transects the southwestern part of the EEP (Chekunov et al., 1992; Stephenson et al., 1993). It is bounded by two Precambrian basement massifs, the Ukrainian Shield to the north and the Voronezh Massif to the south, which together define a domal structure, some 1000 km in diameter, transected by the rift (Fig. 1). The PDD probably evolved during the Late Devonian by northwestward rift propagation from the Peri-Caspian area. Prior to the onset of crustal extension, the Ukrainian Shield and the Voronezh Massif were partially covered by marine Middle Devonian sediments (Nikishin et al., 1996; Alekseev et al., 1996). Broad lithospheric doming of the rift flanks, accompanied by voluminous magmatic activity, probably commenced shortly after the onset of rifting. Constraints on the timing of basement uplift are provided by detailed stratigraphic studies of the Devonian sedimentary succession in the Voronezh Massif and the Moscow Syneclise to the north (Alekseev et al., 1996). A regional erosional event spanning the Frasnian and Famennian boundary may mark the timing of maximum uplift. The onset of uplift may have commenced in the mid-Frasnian (Rechitsian) (Fig. 2).

Excellent constraints on the 3D geometry of the rift are provided by a dense grid of seismic reflection profiles and 14 deep seismic sounding (DSS) lines,

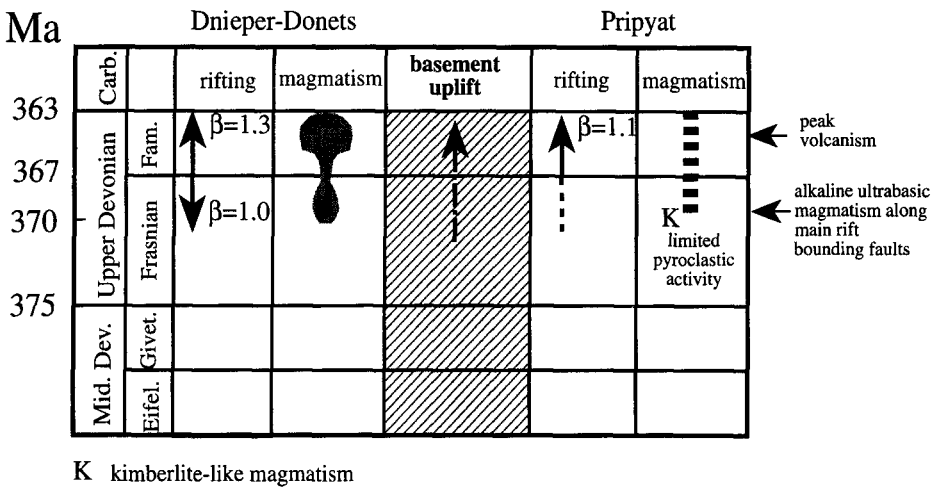

Fig. 2. Timing of rifting, magmatism and basement uplift in the Dnieper–Donets and Pripyat segments of the rift. Timing of rifting and β factors from Kusznir et al., 1996a,b). Timescale from Harland et al. (1990).

which allow good resolution of the structure of the lower crust and Moho (e.g., Stephenson et al., 1993). In addition, an extensive programme of deep drilling by the former Soviet petroleum industry provides a unique dataset for investigating the three-dimensional geometry of the magmatic and sedimentary fill of the rift and also an opportunity to sample sub-surface magmatic rocks. The Dnieper–Donets segment of the rift is characterised by linear bounding faults penetrating much of the crust, significant crustal thinning ($\beta \sim 1.3$; Kusznir et al., 1996a) and abundant syn-rift volcanic activity. In the westernmost part of the rift, the Pripyat Trough forms a separate sub-basin, characterised by much smaller amounts of extension (maximum $\beta = 1.12$; Kusznir et al., 1996b). The Pripyat Trough is separated from the main Dnieper–Donets rift by a volcanic ridge (Ulmishek et al., 1994), which will be referred to as the Braguin–Loev Saddle in subsequent sections.

The evolution of the PDD rift was contemporaneous with the development of a major back-arc rift system in Western and Central Europe (Ziegler, 1990). The main extensional phase of the Dnieper–Donets segment occurred between the late Frasnian (370 Ma) and the end of the Devonian (363 Ma) (Kusznir et al., 1996a; Fig. 2). Rifting was accompanied by intense volcanic activity. In the Pripyat Trough over two thirds of the rifting occurred extremely rapidly between 367–364 Ma (Kusznir et al., 1996b), with little associated magmatic activity outside the Braguin–Loev Saddle. Local occurrences of pyroclastic deposits within this sub-basin are most likely the result of air fall deposition. A cluster of volcanic diatremes, which have some geochemical and mineralogical affinity to kimberlites, occurs on the northern flanks of the Pripyat Trough (Fig. 1).

Pre-rift sedimentation was characterised by shallow marine facies. Within the lower part of the syn-rift sequence, major salt deposits suggest that the palaeoenvironment may have been a restricted marine basin similar to the present-day Red Sea. This salt horizon was extensively remobilised between the Late Devonian and Early Permian, resulting in abundant salt diapirs throughout the basin. The salt diapirs locally exhume fragments of mafic igneous rocks from deeper levels of the basin fill. The Frasnian–Famennian succession contains interbedded clastic and carbonate sediments, salt and volcanic and volcaniclastic rocks (Kusznir et al., 1996a,b).

3. Volcanic activity associated with the PDD rift

The distribution of volcanism within the PDD rift is strongly controlled by the pre-existing basement structure, as is the segmentation of the basin from northwest to southeast into the relatively shallow Pripyat Trough, the much deeper Dnieper segment and the partly inverted Donbas–Donets Basin. There are major changes in the crustal structure, thickness,

deformation and metamorphic history of the sedimentary fill and the intensity of syn-rift volcanic activity along the length of the rift (Chekunov et al., 1992). Basin evolution was affected by compressional tectonics during the Permian, related to the Uralian orogeny; the degree of deformation increases markedly from northwest to southeast. Within the axial zone of the Dnieper segment of the rift the crust is thinned to 30–35 km from 40–45 km on the adjacent flanks (Chekunov et al., 1992). The syn-rift and post-rift sedimentary succession is more than 20 km thick in the Donets segment, overlying a highly attenuated crust (ca. 20 km thick) inferred to be predominantly mafic on the basis of seismic data.

Late Devonian (Frasnian and Famennian) magmatic activity, predominantly consisting of alkaline–ultramafic lavas, alkali basalts and their differentiates, occurred mainly along major syn-rift fault systems, particularly at their intersection with older basement faults. It is probable that only a comparatively small volume of magma was erupted, the rest being emplaced within the crust as sills/dykes and as an extensive mafic crustal underplate (Wilson, 1993a). The latter is imaged in many of the deep seismic lines across the basin as a high velocity layer at the base of the crust (e.g., Stephenson et al., 1993). The volume of basic and ultrabasic magmas emplaced into the lower crust may have been sufficient to induce melting of the lower crust, providing an additional mechanism for crustal thinning in addition to lithospheric extension.

Over the period 1992–1995, a detailed study of the volcanism of the Pripyat and Dnieper segments of the PDD rift was undertaken to characterise the age, distribution and geochemical characteristics of the volcanic activity, and to assess the relative roles of lithospheric and asthenospheric mantle source components in the petrogenesis of the most primitive basic and ultrabasic magmas. All available well logs were compiled and correlated to evaluate the distribution of magmatic activity within the basin. Maps were prepared based on these data for the Frasnian and Famennian stages showing the distribution and characteristics of volcanism within the Dnieper–Donets segment of the basin and the Braguin–Loev Saddle which separates it from the adjacent Pripyat Trough. Concurrently, representative samples of the most primitive basic and ultrabasic magmatic rocks were selected for major- and trace-element and Sr–Nd isotopic analysis. These data provide a basis for explaining the petrogenesis of the magmas in the context of the geodynamic setting of the EEP. Integration of the petrogenetic model with the results of dynamic modelling studies of the rift (e.g., Kusznir et al., 1996a,b; van Wees et al., 1996) provide important new insights into the geodynamics of basin formation.

de Boorder et al. (1996) include a brief summary of the magatism of the Donets segment of the rift. The southern boundary fault of this rift segment provides a focus for the emplacement of Middle to Late Devonian alkaline ultramafic and basaltic stocks, flows and breccias. In addition, Late Devonian flows of tholeiitic basalts are reported, associated with deep fault zones in the central and northern parts of the basin. A unique aspect of the Donets segment of the rift, compared to those rift segments further north, appears to be the periodic rejuvenation of magmatic activity from mid-Carboniferous–Late Jurassic times.

3.1. Distribution of magmatic rocks within the basin

The large number of deep and super-deep exploration wells drilled within the PDD rift as part of the programme of oil and gas exploration provide a unique opportunity to study the sub-surface Late Devonian volcanic succession. The chronology of the volcanic sequence is well constrained palaeontologically but there are no reliable absolute age controls by radiometric dating. The generally high degree of alteration of the samples (loss on ignition $\gg 2\%$) precludes the possibility of obtaining meaningful ages by K–Ar dating. A collaborative programme of whole rock laser ^{40}Ar–^{39}Ar dating of Palaeozoic magmatic rocks from the EEP has been established with J. Wibrans of the Free University Amsterdam, but thus far no ages are available for the PDD rift.

Reconstruction of the distribution of the volcanism within the basin is based on data from nearly 300 deep wells which intersect the volcanic succession. Fig. 3 illustrates the distribution and types of Frasnian and Famennian magmatic activity within the Dnieper–Donets segment. Fig. 4 shows the variation in thickness of the volcanic sequence (both lava flows and pyroclastics).

Two distinct volcanic sequences have been recognised within the basin fill, of late Frasnian and late Famennian age, respectively (Fig. 2). The lower sequence consists predominantly of basalts, pyroclastics and alkali–ultramafic breccias and agglomerates, whilst the upper sequence is characterised by basaltic, trachytic and rhyolitic lavas. Dolerite dykes are widespread and small stocks of gabbro-dolerite also occur. The volume of magmatic rocks is estimated to be 7200 km^3, equal to about 25% of the volume of the Devonian sequence within the Dnieper–Donets depression. The volcanics reach a maximum thickness of 2.7 km, located at depths between 3 and 12 km below the surface. They are overlain by Late Devonian and Carboniferous terrigenous clastics.

The available well data provide good control on the distribution of volcanism in the northwest and central parts of the Dnieper–Donets depression and in the volcanic Bragin–Loev Saddle which separates it from the Pripyat Trough. Our knowledge of the distribution of volcanic rocks in the southwestern part of this rift segment is, however, poor because the volcanic horizons are located at great depths and are rarely penetrated by exploration wells. Salt diapirs occasionally exhume fragments of dolerite of unknown age from deeper horizons.

3.2. Late Frasnian volcanism

The lower volcanic sequence covers an area of about 9400 km^2, with a volume of about 1800 km^3. Magmatism is focussed on the Braguin–Loev and Belotserkovsky highs, along the northern boundary fault of the rift and within the uplifted Priluksko–Ichnjansky block (Fig. 3). The thickness of the volcanics ranges from 100 to 900 m, with an average of 300 m. Basalts, tuffs and alkali–ultramafic agglomerates predominate. Analysed samples include alkali basalts, basanites, nephelinites, mica-bearing picrites and trachytes. Explosive volcanism was common at this stage, with pyroclastic rocks accounting for 70–90% of the volcanic products. At least ten discrete volcanic centres have been identified based upon the distribution of volcanic facies and thickness variations. The volcanic edifices are composed of lavas, intercalated with agglomerate, agglutinate and tuffs. Away from the volcanic centres, contemporaneous deposits include intercalated volcaniclastic and terrigenous sediments.

3.3. Late Famennian volcanism

The upper volcanic sequence covers an area of nearly 9800 km^2 (Fig. 3) within the central part of the Braguin–Loev transverse saddle, the Prilusko–Ichnjansky block, along the axial part of the rift and, particularly, along the northern boundary fault. The volcanic sequence averages 300–500 m in thickness and is locally more than 2000 m thick because of the development of localised stratovolcanoes. The main forms of volcanic activity which can be recognised include lava flows, tuffs, pyroclastic flow breccias, explosion pipes and volcanic necks. In terms of their chemical composition, basalts, trachytes and rhyolites predominate. Some wells penetrate highly reddened lavas, which may indicate subaerial emplacement, whilst in other wells pillow lavas intercalated with argillites indicate subaqueous eruptions. Pyroclastic activity was much less common than in the lower volcanic sequence, accounting for only 25–35% of the volcanic products. The volcanic centres appear to be concentrated along both longitudinal and transverse fault systems. In some cases they were coincident with the eruption centres of the late Frasnian volcanic phase. The volume of volcanic material accumulated during the late Famennian (5400 km^3) was approximately three times greater than that emplaced during the Frasnian phase.

3.4. Hypabyssal intrusions

Coarse-grained, gabbro-dolerite stock-like intrusions occur at scattered localities throughout the basin. These have discordant contacts with the surrounding Devonian terrigenous sediments, which exhibit hornfels-facies metamorphism and hydrothermal alteration (Fig. 3). In addition, there appears to have been widespread intrusion of tholeiitic dolerite dykes and sills, synchronous with the Late Devonian volcanism. The gabbro-dolerite intrusions cross-cut formations ranging from Frasnian to later Famennian in age. It is, however, difficult to constrain their absolute age and therefore they are shown on both the Frasnian and Famennian maps. The sheet-like intrusions range from 0.2 to 250 m in thickness, most

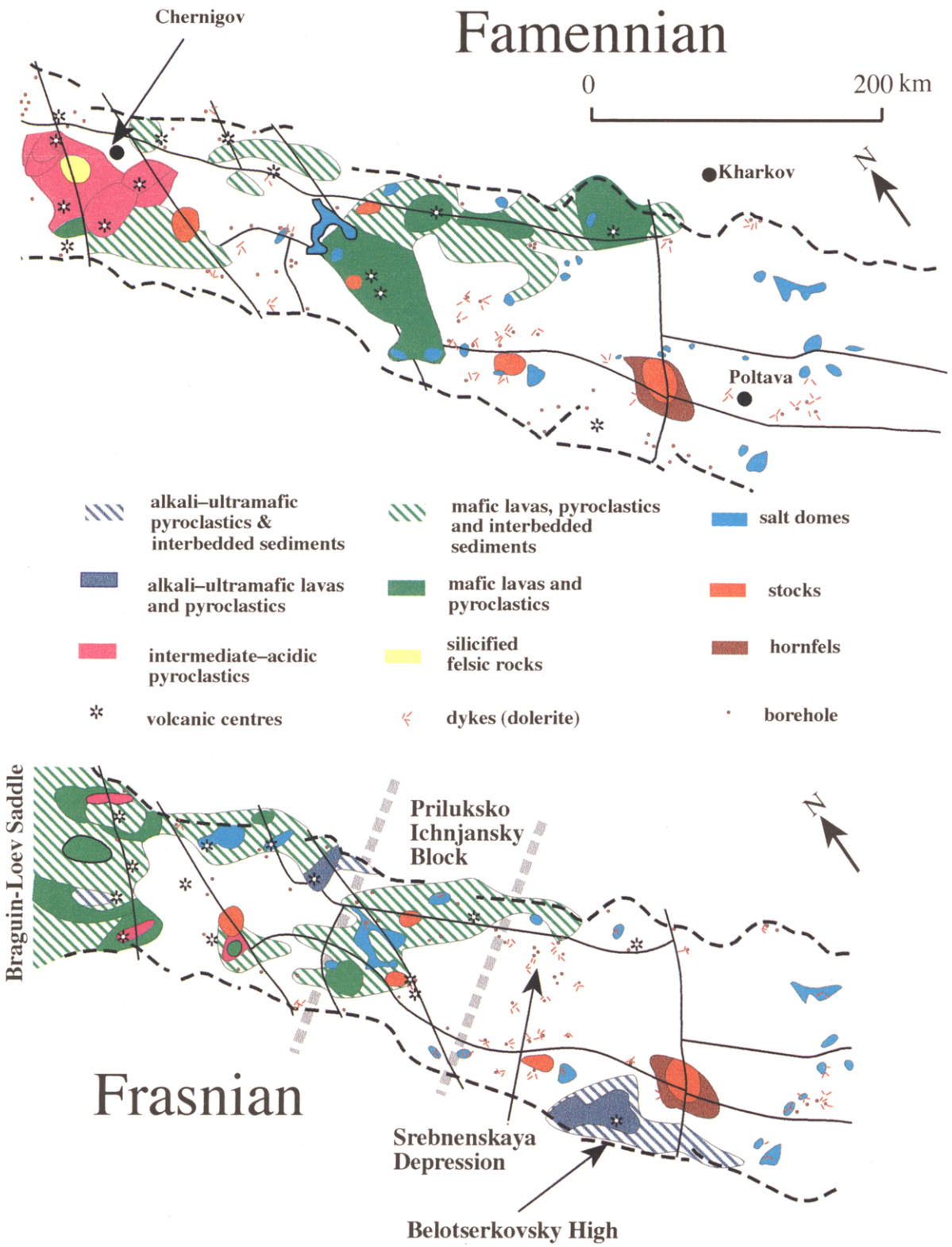

Fig. 3. Maps showing the distribution of magmatism in the Dnieper–Donets segment of the rift during the Frasnian and Famennian.

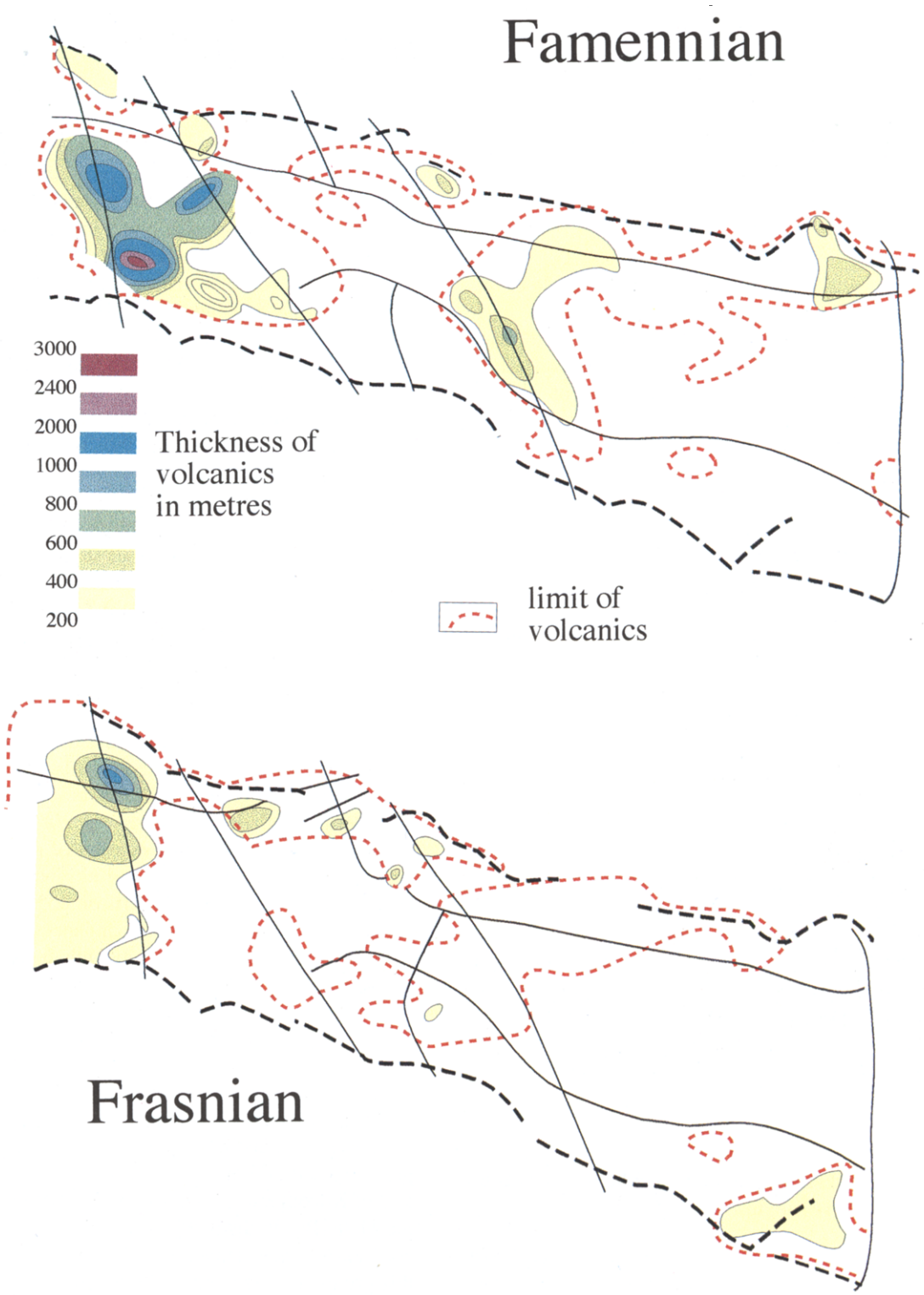

Fig. 4. Maps showing the thickness and areal distribution of Frasnian and Famennian volcanics in the Dnieper–Donets segment of the rift.

typically 10–25 m. They intrude both the central volcanic complexes and the surrounding sediments and also occur as fragments in salt diapirs. Dykes are particularly concentrated within one of the major depocentres within the basin, the Srebnenskaya depression (Fig. 3).

3.5. Kimberlites

An extensive diatreme field (Zhlobin Saddle) has been identified on the northern flanks of the Pripyat depression which was originally thought to have kimberlite affinities. This has been extensively studied by Belarussian geologists because of its diamond-bearing potential. On the basis of preliminary geochemical data obtained as part of this study, however, it appears that these are alkali ultrabasic diatremes rather than true kimberlites. The age of the diatremes is well constrained stratigraphically to the lowermost Rechitsian horizon of the middle Frasnian (ca. 371 Ma; Kusznir et al., 1996b; E.A. Nikitin (BelNIGRI), pers. commun., 1995). Magmatism is therefore concurrent with the onset of rifting in the Pripyat Trough.

3.6. Voronezh Massif

Devonian volcanic rocks outcrop on the northern flank of the Dnieper–Donets rift in the south eastern part of the Precambrian Voronezh Massif. Kimberlitic breccias containing fragments of peridotite and pyroxenite have been reported, in association with Late Devonian plateau basalts (Gon'shakova et al., 1967). Unfortunately the Voronezh Massif is difficult to access and no samples of the magmatic rocks could be obtained for this study. Major element analyses the basalts, obtained by wet chemical techniques (Gladkikh, 1971), indicate that the plateau basalts are tholeiites comparable in composition to the dolerite dykes and sills which occur throughout the PDD rift.

4. Major- and trace-element geochemistry of the most primitive magmas

Whole-rock, major- and trace-element analyses of over 100 samples of magmatic rocks from the PDD rift were obtained by XRF at Leeds. Many of the samples analysed were intensely altered and were therefore considered unsuitable for further analysis. The XRF data were used to select the freshest and most primitive (least differentiated) samples for subsequent REE analysis by ICP–AES and Sr–Nd isotope analysis, based on loss on ignition <5–8% and MgO content >7%. Representative major- and trace-element analyses are given in Tables 1 and 2 and Sr–Nd isotope data in Table 3.

The samples have been classified based upon their position in the total alkalis ($Na_2O + K_2O$) versus silica diagram (TAS, Fig. 5) and in a plot of SiO_2 versus Nb/Y (Fig. 6). The latter diagram was used to minimise problems caused by the mobility of Na and K in altered samples. Both diagrams result in similar classifications. All analyses were plotted on a volatile free basis (renormalised to 100%) to account for the variable loss on ignition (LOI). The most primitive magmas range in composition from subalkaline tholeiitic basalts (primarily dolerite dykes and basalts from the Voronezh Massif) to alkali basalts, basanites, nephelinites and alkali picrites. Some of the most highly magnesian samples from the Pripyat Trough (e.g., OOP1B, OOP2) have clearly accumulated olivine, indicated by their high Ni contents (>700 ppm).

The trace-element characteristics of selected samples are presented as mantle-normalised trace-element variation diagrams in Fig. 7. These indicate that the doleritic (diabase) intrusions (e.g. 2058) are likely to be the products of higher degrees of partial melting than the associated basic and ultrabasic alkaline lavas. The trace-element pattern of 2058 is almost flat at 10× primordial mantle abundances, consistent with its derivation by a relatively high degree of partial melting (10%) from a mantle source with near-primordial trace-element abundances. Samples from the Pripyat Trough (Braguin–Loev Saddle) have been divided into two groups: potassic samples (Fig. 7a), including the supposed kimberlite-like samples PK1 and PK501, and sodic samples (Fig. 7b). The sodic samples have a distinct negative K anomaly which is probably real, although there could have been some loss of K from these samples during alteration. Sample OOP1B has distinctly lower abundances of incompatible trace elements than the other samples in this group. This is likely to be a consequence of the accumulation of excess olivine in this sample (40%)

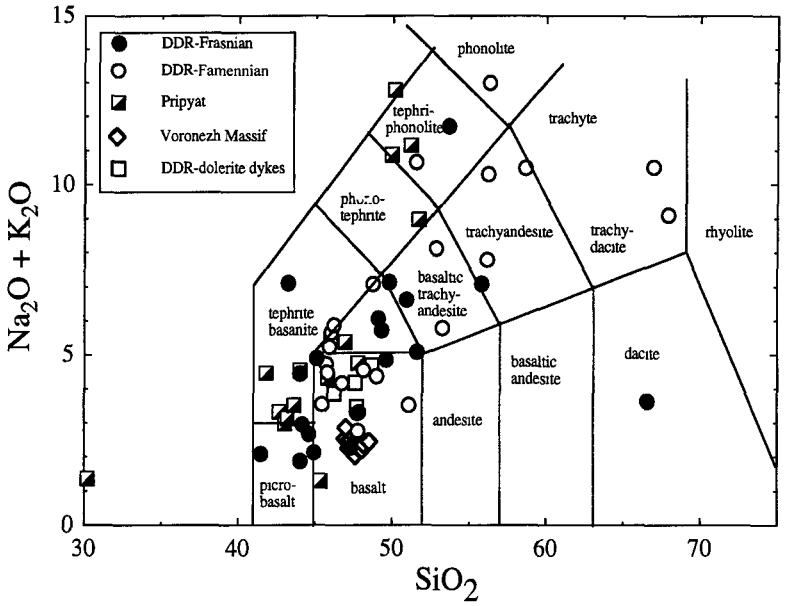

Fig. 5. Total alkalis ($Na_2O + K_2O$) versus SiO_2 diagram showing the chemical classification of the magmatic rocks. After Le Bas et al. (1992).

which will have a dilution effect on the trace-element abundances. The trace-element patterns of the sodic alkali basalts and basanites (Fig. 7b,c) show strong similarities to those of HIMU oceanic island basalts (Wilson, 1993b) which are generally accepted to be related to the activity of mantle plumes.

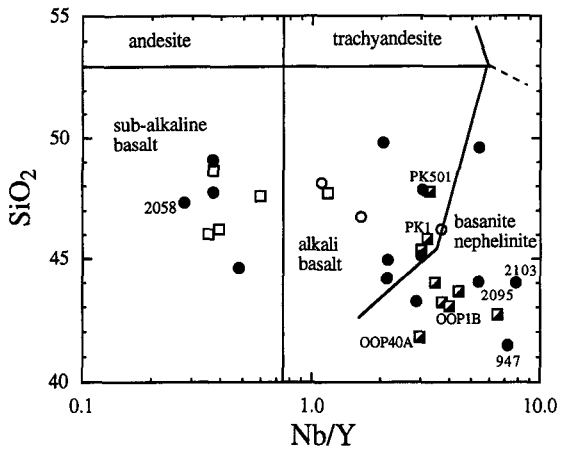

Fig. 6. SiO_2 versus Nb/Y classification diagram (after Winchester and Floyd, 1977). Data sources: Pripyat and Dnieper–Donets samples (this study and M. Wilson, unpublished data); Voronezh Massif (Gladkikh, 1971). Representative analyses of primitive basic and ultrabasic samples given in Tables 1 and 2.

Fig. 8 shows the variation of Nb/Y versus Zr/Y for the most primitive basic and ultrabasic samples. This diagram is relatively insensitive to the effects of alteration, fractional crystallization and variable degrees of partial melting (Fitton et al., 1996). The linear trend suggests that at least two different source components were involved in the petrogenesis of the magmas. Low Zr/Y and Nb/Y ratios could indicate the involvement of either a depleted upper mantle (DM) or a primordial (PM), possibly lower mantle, source component. In contrast, high Zr/Y and Nb/Y ratios are consistent with the involvement of an enriched mantle source component which may reside within a geochemically distinct mantle plume.

4.1. Sr–Nd isotope data

The Sr–Nd isotopic compositions of nine samples, selected to reflect the major chemical variations within the PDD magmatic suite, are given in Table 3. Samples were leached prior to analysis in an attempt to minimise the effects of low-temperature alteration, as described in the footnote to Table 3. The isotopic data, plotted in Fig. 9 (age corrected to 370 Ma), define a steep array between depleted mantle (DM) and bulk-earth-like (BE) isotopic compositions. The Sr–

Table 1
Representative major- and trace-element analyses of basic and ultrabasic igneous rocks from the Dnieper–Donets segment of the PDD rift

	2058	2095	604	951	947	49	2103	438	800	1126
SiO_2	47.32	44.04	45.10	51.59	41.47	49.81	44.00	48.66	46.73	45.47
TiO_2	1.40	3.72	3.24	2.84	5.93	2.62	4.27	2.16	2.18	2.11
Al_2O_3	14.34	8.69	11.70	14.04	3.97	14.77	8.50	14.14	14.65	15.47
Fe_2O_3	11.31	17.17	14.63	10.23	21.09	12.66	15.38	13.25	13.05	17.27
MnO	0.18	0.35	0.21	0.22	0.30	0.21	0.39	0.37	0.31	0.27
MgO	9.76	15.04	9.52	7.01	14.38	7.24	11.11	8.32	7.93	5.83
CaO	13.29	8.42	10.07	8.50	10.00	4.87	11.25	8.22	10.57	9.77
Na_2O	2.06	1.19	2.98	4.16	1.09	4.25	1.57	3.60	2.96	3.19
K_2O	0.22	0.68	1.92	0.92	1.00	2.89	2.88	1.09	1.21	0.36
P_2O_5	0.11	0.68	0.64	0.50	0.75	0.67	0.64	0.22	0.41	0.27
LOI	4.12	6.11	2.22	2.97	2.62	2.74	3.03	2.08	4.04	1.85
Ni	166	199	165	40	131	89	167	137	83	42
Cr	420	207	246	28	71	156	217	245	86	117
V	259	264	306	409	351	254	234	374	265	352
Sc	39	21	21	22	30	17	12	40	26	42
Cu	120	42	61	153	174	56	339	134	82	45
Zn	70	242	136	267	464	162	257	106	69	68
Sr	246	977	1051	542	1055	996	1893	759	823	371
Rb	5	13	36	22	45	50	42	24	37	3
Ba	79	820	970	1076	626	1128	2795	321	444	296
Zr	69	361	239	138	629	238	261	105	133	102
Nb	5	129	66	41	201	51	118	10	36	19
Y	18	24	22	23	28	25	15	27	22	21
La	7.1	90.4							35.3	18.2
Ce	17.2	205.3							77.5	40
Nd	10.8	78							32	19.3
Sm	3.15	12.79							6.4	4.34
Eu	1.19	3.61							2.01	1.68
Gd	4.13	9.5							6.13	4.86
Dy	3.65	5.18							4.46	3.92
Er	2.05	2.09							2.23	2.16
Yb	1.91	1.87							2.05	2.08

Sample	Rock type	Drill hole location	Depth	Age
2058	dolerite	Salogubovskaya-388	5538 m	Frasnian
2095	ultramafic lava	Severo-Zagorovskaya-1	4706 m	Frasnian
604	ankaramite	Sednevskaya-310	3403 m	Frasnian
951	alkali basalt	Kinashevskaya-1	3647 m	Frasnian
947	ultramafic lava	Belotserkovskaya-231	1902 m	Frasnian
49	alkali basalt	Brusilovskaya-2	2598 m	Frasnian
2103	ultramafic lava	Severo-Zagorovskaya-1	4769 m	Frasnian
438	dolerite	Hole 6053 Dmitrievskiy Salt Dome	273 m	unconstrained
800	dolerite	Krasno-Partizanskaya-4	3746 m	Famennian
1126	alkali basalt	Kukshin-1	3210 m	Famennian

Analyses by XRF at Leeds University; major elements normalised to 100% volatile free. REE by ICP at RHUL (University of London). LOI = loss on ignition.

Table 2
Representative major- and trace-element analyses of basic and ultrabasic igneous rocks from the Pripyat segment

	Minsk1	Minsk3	Minsk4	Minsk8	OOP1B	OOP2	OOP23	OOP40a	PK501	PK1
SiO_2	44.01	30.22	45.34	42.69	43.04	43.20	51.16	41.79	47.77	45.82
TiO_2	3.05	5.00	2.37	4.10	2.61	2.58	1.62	3.68	1.80	1.81
Al_2O_3	12.22	10.54	8.84	9.35	7.61	7.56	17.95	11.25	10.09	11.07
Fe_2O_3	16.21	27.46	14.60	16.36	14.87	14.84	11.13	17.07	13.73	13.12
MnO	0.09	0.51	0.17	0.35	0.20	0.20	0.45	0.14	0.18	0.14
MgO	16.21	14.12	16.44	9.98	18.70	18.68	2.93	9.55	13.26	17.91
CaO	2.95	9.66	10.28	12.98	9.48	9.28	3.39	11.19	7.86	5.36
Na_2O	0.61	1.17	0.98	1.98	2.12	2.20	9.63	0.92	2.23	0.33
K_2O	3.93	0.20	0.32	1.34	0.85	0.93	1.52	3.54	2.53	3.98
P_2O_5	0.71	1.13	0.66	0.88	0.52	0.52	0.21	0.86	0.56	0.48
Total	99.99	100.01	100.00	100.01	100.00	99.99	99.99	99.99	100.01	100.02
LOI	7.0	6.5	8.79	2.85	2.41	2.63	7.07	5.05	+1.0	8.33
Ni	103	392	537	122	789	817	nd	56	166	93
Cr	245	294	602	106	829	784	21	51	222	297
V	386	597	289	350	225	204	715	395	290	270
Sc	34	42	23	25	19	19	nd	26	21	25
Cu	148	380	176	642	152	121	13	248	224	217
Zn	58	595	222	140	104	99	250	89	128	62
Sr	397	1925	538	1295	938	887	821	1076	868	346
Rb	55	2	11	45	13	12	125	56	45	61
Ba	1375	5502	584	645	769	758	2045	1026	1043	214
Zr	215	265	130	336	173	174	574	189	86	113
Nb	66	123	45	169	64	63	169	68	46	48
Th	12	17	7	22	12	11	6	13	9	6
Y	19	26	15	26	16	17	12	23	14	15
La	62	89.2	40.6	101.4	59.4	59.5	62.4	62.2	41.5	39.3
Ce	131.1	182	87.2	213.5	123.1	123.6	81.6	128.6	85.7	81.8
Nd	51.6	66.5	35.7	81.5	48	47.8	18.6	54.4	30.1	29.4
Sm	9.15	11.66	6.64	14.93	8.26	8.26	2.75	10.0	5.16	5.23
Eu	2.6	3.36	2.04	4.93	2.4	2.41	0.79	2.97	1.53	1.56
Gd	7.26	9.32	5.52	11.9	6.37	6.4	2.5	8.17	4.4	4.39
Dy	4.45	5.89	3.48	6.89	4.02	4.02	2.15	5.25	2.99	3.22
Er	1.9	2.28	1.43	2.58	1.32	1.32	1.01	1.76	1.42	1.27
Yb	1.64	1.86	1.17	2.11	1.16	1.17	1.26	1.46	1.32	1.18

Sample	Rock type	Drill hole location	Depth	Age
Minsk1	lamprophyre	Dneprovskaya	3565 m	Frasnian–Famennian
Minsk3	ultramafic lava	Krasnoselskaya 210	3360 m	Frasnian–Famennian
Minsk4	ultramafic lava	East Borschevka 3	2925 m	Frasnian–Famennian
Minsk8	alkali basalt dyke	Borschevska-4	2125 m	Frasnian–Famennian
OOP1B *	ultramafic lava	Braguin–Loev Saddle	1274 m	Frasnian–Famennian
OOP2 *	ultramafic lava	Braguin–Loev Saddle	1282 m	Frasnian–Famennian
OOP23	phono-tephrite	Braguin–Loev Saddle	570 m	Frasnian–Famennian
OOP40a	lamprophyre	Braguin–Loev Saddle	4515 m	Frasnian–Famennian
PK501	?kimberlite	N.rift shoulder	near surface	Frasnian
PK1	?kimberlite	N.rift shoulder	373–555 m	Frasnian

Analyses by XRF at Leeds University. Major elements normalised to 100% volatile free. REE by ICP at RHUL (University of London). LOI = loss on ignition; nd = not detected.
* Samples from the same flow unit.

Table 3
Sr–Nd isotopic compositions

Sample	Rb/Sr	$^{87}Sr/^{86}Sr$ measured	$^{87}Sr/^{86}Sr$ 370 Ma	Sm/Nd	$^{143}Nd/^{144}Nd$ measured	$^{143}Nd/^{144}Nd$ 370 Ma
OOP1 *	0.0333	0.70398	0.70348	0.171	0.51256	0.51231
OOP1B	0.0139	0.70403	0.70382	0.172	0.51258	0.51232
OOP2	0.0135	0.70394	0.70373	0.173	0.51252	0.51226
OOP23	0.1523	0.70560	0.70328	0.148	0.51263	0.51241
OOP40A	0.052	0.70555	0.70476	0.184	0.51255	0.51228
PK501	0.0518	0.70551	0.70472	0.171	0.51237	0.51211
PK1	0.1763	0.72016	0.71747	0.178	0.51254	0.51228
2058	0.0203	0.70281	0.70250	0.292	0.51305	0.51263
1126	0.0081	0.70457	0.70445	0.225	0.51276	0.51243

* Analysis of second sample from the same core as OOP1B.

Nd–Sr isotopic compositions were measured on ~150 mg of whole-rock powders leached in 2.5M HCl for 4 h at 50°C to minimise the effects of any post-emplacement alteration. Sr and Nd were analysed using a technique modified from Gerlach et al. (1987). Sr was run on a VG 54E Isomass mass spectrometer and Nd on a VG MM30 mass spectrometer, both at the University of Leeds. Nd isotopic compositions are normalised to $^{146}Nd/^{144}Nd = 0.7219$ and Sr isotopic compositions to $^{86}Sr/^{88}Sr = 0.1194$. Values are relative to the following standards: NBS987 = 0.71025; La Jolla = 0.51186.

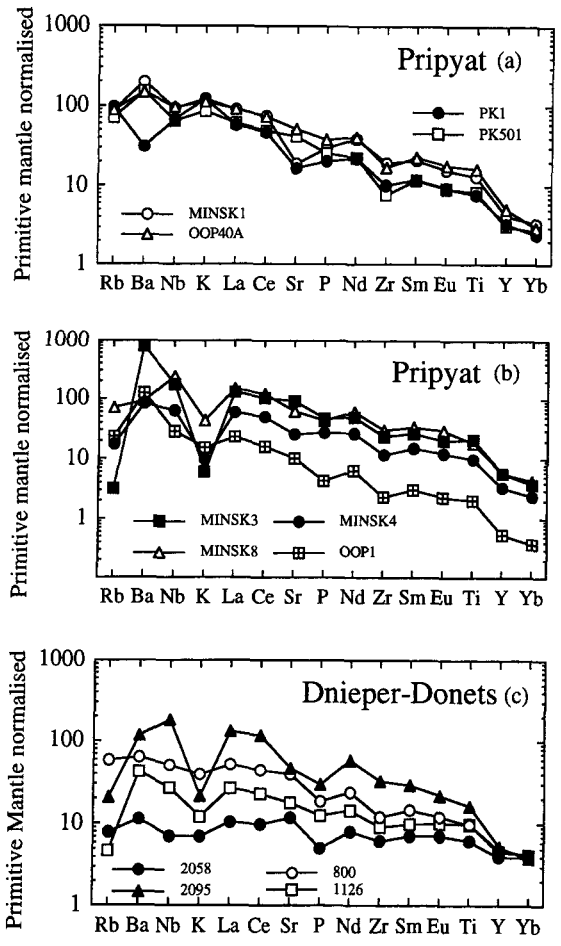

Fig. 7. Primitive-mantle-normalised trace element variation diagrams for primitive basic and ultrabasic magmatic rocks. (a) Pripyat potassic samples with $K_2O/Na_2O > 1$ (weight ratio). (b) Pripyat sodic samples with $K_2O/Na_2O < 1$ (weight ratio). (c) Dnieper–Donets samples. Data from Tables 1 and 2. Normalisation constants from Sun and McDonough (1989)

Nd isotopic data correlate with major-element composition. The tholeiitic dolerite sample 2058 has the most depleted Sr–Nd isotope composition. This suggests that the highest-degree partial melts (tholeiites) have the highest contribution from the depleted mantle source component. The kimberlite-like sample PK1 has a much more radiogenic Sr isotopic composition than the other samples which suggests that, for this sample, the leaching procedure was insufficient to remove the effects of alteration. Alternatively the high $^{87}Sr/^{86}Sr$ ratio might reflect the incorporation of crustal fragments, although these would have to have a similar Nd isotopic composition to the host magma. The other kimberlite-like sample PK501 has the most enriched Sr–Nd isotopic composition of all the samples and may be derived from an enriched zone within the continental lithospheric mantle.

Comparison of the Sr–Nd isotopic compositions of the majority of the PDD samples analysed with that of syenites, ijolites, carbonatites and kimberlites from the contemporaneous 370 Ma alkaline Kola Peninsula magmatic province (Mahotkin and

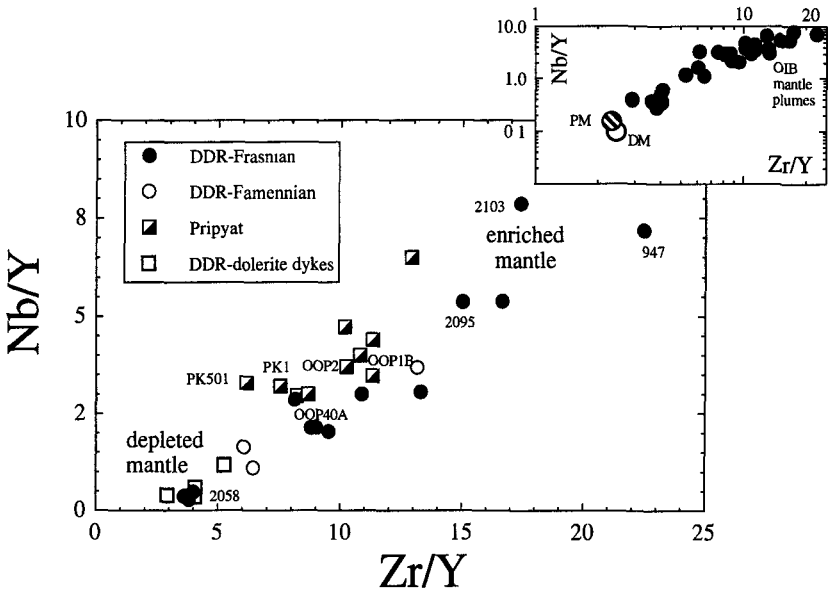

Fig. 8. Variation of Nb/Y versus Zr/Y for the most primitive basic and ultrabasic magmatic rocks. Inset shows the same data plotted on a logarithmic scale for comparison with estimates of these ratios in depleted (*DM*) and primitive (*PM*) mantle sources from Sun and McDonough (1989).

Juravlev, 1993; Kramm and Kogarko, 1994; Zaitsev and Bell, 1995; Fig. 1) reveals a strong similarity.

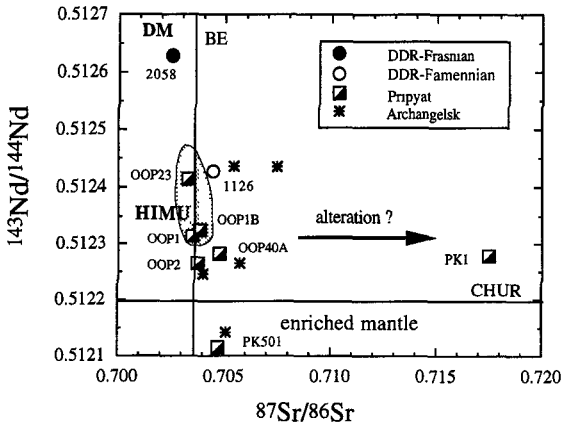

Fig. 9. Variation of $^{143}Nd/^{144}Nd$ versus $^{87}Sr/^{86}Sr$ (initial ratios at 370 Ma) for selected basic and ultrabasic samples from Tables 1 and 2. Data given in Table 3. Shown for comparison is the Nd–Sr isotopic composition of 370 Ma syenites, ijolites and carbonatites from the Kola Peninsula, Russia (grey shaded field); data from Kramm and Kogarko (1994) and Zaitsev and Bell (1995). Also plotted are the Nd–Sr isotopic compositions of 367 Ma kimberlites and melilitites from the Archangelsk region (asterisks; Mahotkin and Juravlev, 1993). Mantle reservoirs: depleted mantle (*DM*), HIMU, Bulk Earth (*BE*) and CHUR are calculated values at 370 Ma.

The data cluster close to the Sr–Nd isotopic composition of the mantle source of HIMU-oceanic island basalts (Wilson, 1993b) at 370 Ma. This may indicate the involvement of a common, sub-lithospheric, mantle source component beneath the two magmatic provinces which may be plume related.

5. Discussion

5.1. Relationship between magmatism and lithospheric extension

The occurrence of volcanism during continental rifting is often attributed to adiabatic decompression melting of the asthenosphere during lithospheric extension (e.g., McKenzie and Bickle, 1988; White and McKenzie, 1989). If the mantle (both lithosphere and asthenosphere) beneath the EEP was predominantly anhydrous (i.e. volatile free) during the Late Devonian, then, in terms of Fig. 10, it is clear that a β factor of only 1.3 (as deduced for the DDR rift by Kusznir et al. (1996a) would be inadequate to explain the high degrees of melting observed, as the anhydrous mantle solidus is only just overstepped (black shaded region) for mantle potential temperatures 300°C above normal, assum-

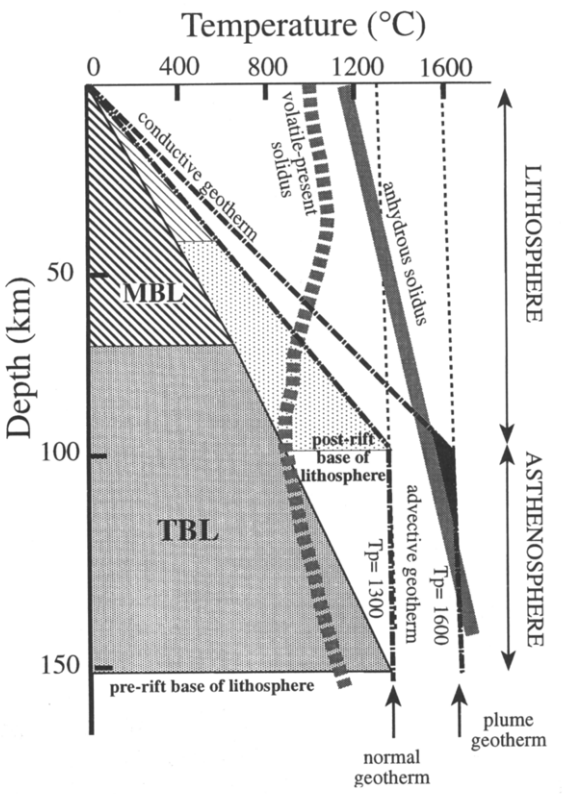

Fig. 10. Schematic temperature–depth diagram showing the location of geothermal gradients for mantle potential temperatures of 1300 and 1600°C in relation to the position of the anhydrous (volatile-free) and volatile-saturated mantle solidus. Modified after Wilson (1993a). *MBL* = mechanical boundary layer; *TBL* = thermal boundary layer. In the example illustrated the initial lithospheric thickness is 150 km. After extension (β = 1.3; the maximum stretching in the Dnieper–Donets rift segment) the thinned base of the lithosphere is at 100 km depth. If the mantle is volatile free, partial melting (black shaded area) will only occur where the geotherm oversteps the anhydrous solidus for mantle potential temperatures in excess of ca. 200°C above ambient (1300°C). If the base of the lithosphere (TBL) is enriched in volatiles, however, partial melting may occur at low degrees of extension and normal potential temperatures. The initial volatile-enriched partial melts are likely to escape rapidly from the system such that subsequent partial melting would take place along the anhydrous solidus. Thus to generate large amounts of partial melt beneath thick lithosphere appears to require the presence of thermally anomalous mantle, i.e. a mantle plume.

ing a pre-rift lithospheric thickness of 150 km. This provides a particularly important constraint during the early stages of rifting in the late Frasnian when the β factor must have been close to 1. If, however, the lower parts of the lithosphere and/or the asthenosphere were volatile (H_2O–CO_2) enriched, then partial melting along the 'volatile-present' mantle solidus could have generated fairly large amounts of partial melt, without any requirement for the involvement of thermally anomalous mantle, even during the early stages of rifting. Alkali ultrabasic magmas emplaced along the marginal faults of the PDD rift and on the northern flanks of the Pripyat Trough (e.g. PK501) during the Frasnian could have been generated by partial melting of a volatile-enriched zone within the lower lithosphere. The Sr–Nd isotope composition of PK501 (Fig. 9) is consistent with such an interpretation.

It is important to note that the late Famennian volcanic phase is some three times greater in volume than the Late Frasnian phase, coincident with the maximum amount of extension (Fig. 2). Within the Pripyat Trough the most rapid extension occurred within the Famennian (Kusznir et al., 1996b), with over two thirds of the total extension occurring in less than 4 Ma. Here, however, the maximum β factor is only 1.1, which may explain the lack of volcanism in the trough northwest of the Braguin–Loev Saddle. Regardless of whether the mantle (either lithosphere or asthenosphere) was or was not significantly enriched in volatiles, the calculated amount of lithospheric stretching appears inadequate to explain the large amounts of volcanism within the Braguin–Loev Saddle unless the potential temperature of the asthenosphere was significantly elevated above the normal value of 1300°C (Wilson, 1993a). The focus of magmatism within the Braguin–Loev Saddle may be attributed to the presence of a deep basement lineament trending at a high angle to the rift axis which channelled the magmas towards the surface (Chekunov et al., 1992).

Another factor which must be considered, in interpretations of the amount of partial melting, is the extent to which the crustal and mantle parts of the lithosphere deform to the same extent during lithospheric extension. The models of Kusznir et al. (1996a,b) are based on an assumption of uniform stretching. In contrast, van Wees et al. (1996) have explored the effects of greater degrees of sub-crustal lithospheric thinning on the dynamic evolution of the PDD rift. They consider the possibility that, in the southeastern part of the Dnieper–Donets rift, the mantle part of the lithosphere could have been

thinned to less than 30% of its pre-rift thickness, elevating the lithosphere–asthenosphere boundary to ca. 50 km depth. The resultant high degrees of decompression partial melting could explain the generation of tholeiitic basalts in this part of the rift (dolerite dykes and lava flows in the Voronezh Massif and Donbas rift segment). High degrees of thinning of the sub-crustal mantle lithosphere could be attributed, at least in part, to thermal erosion by an ascending mantle plume.

The above constraints, combined with the stratigraphic evidence for a regional uplift event, strongly suggest that the magmatism of the PDD rift was related to the activity of a thermally (and chemically) anomalous mantle plume (e.g., Chekunov et al., 1992). To constrain the timing of plume impact it is clearly important to determine the relative timing of rifting, volcanism and basement uplift. The thermal anomaly /buoyancy flux associated with the plume appears to have generated regional uplift of the order of 300 m prior to or during Frasnian–Famennian rifting (Kusznir et al., 1996a). This is considerable, given that the pre-rift lithospheric thickness is likely to have been at least 150 km. Alekseev et al. (1996) present stratigraphic data which suggest that the uplift of the Voronezh Massif probably commenced in the mid-Frasnian, reaching a maximum at the Frasnian–Famennian boundary. The area seems to have subsided quite rapidly by the Early Carboniferous which may reflect either decay of the plume or the migration of the overriding plate away from its axis. On the basis of the available data summarised in Fig. 2, magmatism and rifting were broadly synchronous, with the main phase of magmatism, in the late Famennian, coincident with the maximum amount of extension.

5.2. Depth of partial melting

Fig. 11 shows the variation of Al_2O_3 versus CaO/Al_2O_3 for primitive basic and ultrabasic igneous rocks from the PDD rift. This diagram has been devised by Herzberg (1995) to estimate the pressures of equilibration of high MgO magmas (>7 wt%) with their mantle source regions based upon the parameterisation of melting experiments on anhydrous mantle peridotite. On the basis of this diagram, it appears that the spectrum of magma

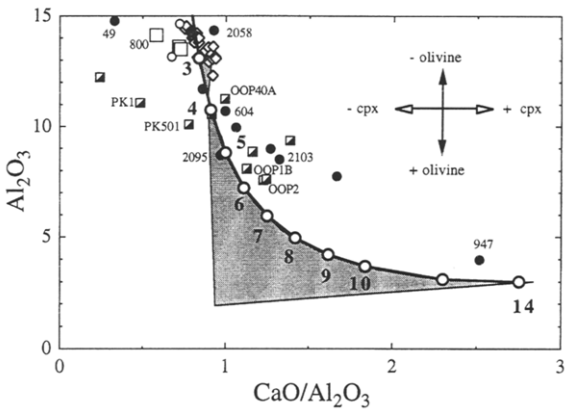

Fig. 11. Variation of Al_2O_3 versus CaO/Al_2O_3 for primitive basic and ultrabasic igneous rocks from the PDD rift. The shaded field depicts the possible range of compositions of primary magmas generated by partial melting of anydrous mantle peridotite, after Herzberg (1995). Bold open circles with numbers indicate the compositions of near-solidus partial melts as a function of pressure in GPa. Vector arrows indicate the effect of addition (crystal accumulation) and subtraction (crystal fractionation) of olivine and clinopyroxene in modifying primitive magma compositions.

compositions in the PDD rift could reflect variable pressures of melting from 5 to 6 GPa (equivalent to 165–200 km depth) for the alkaline ultramafic magmas to 3 GPa (100 km) for the tholeiitic magmas. One sample 947 (Table 1) is distinct from the rest in having a much lower Al_2O_3 content and higher CaO/Al_2O_3 ratio. On the basis of Fig. 11, this magma could have equilibrated at a pressure of 13–14 GPa (equivalent to 400–450 km depth). It is possible, however, that the Ca/Al ratio of this sample has been raised by alteration, in which case the equilibration pressure may be as low as 9 GPa (300 km depth), although its LOI (2.62%) is not unduly high. Either way the data suggest that it is possible that this sample could represent a partial melt generated at depths within the Transition Zone. The presence of the rare mineral moissanite in some of the alkali ultrabasic magmas of the PDD rift confirms their considerable depth of origin.

5.3. Mantle source components

Sample 947, possibly deriving from greater than 400 km depth, has the highest Nb/Y and Zr/Y ratio of the DDR primitive magmas (Fig. 8) and may be closest to a direct partial melt of the enriched mantle

plume source. As discussed previously, in terms of Sr–Nd isotope compositions alone, it is difficult to distinguish between an enriched mantle source component derived from a mantle plume and one which resides in the sub-continental lithospheric mantle. We consider, however, that the combination of the major- and trace-element and Sr–Nd isotope characteristics of the most primitive magmas from the PDD rift provides compelling evidence for the involvement of a chemically distinct mantle plume component in their petrogenesis. In contrast, tholeiite sample 2058, which plots at the opposite end of the trend in Fig. 8, may be the product of partial melting of a depleted upper mantle component, isotopically similar to the source of mid-ocean ridge basalts (MORB) at 370 Ma, at shallower depths (ca. 100 km). The flat primitive-mantle-normalised trace-element pattern of this sample (Fig. 7) indicates either that this source component is not as incompatible-element-depleted as the source of present-day MORB or that its trace-element characteristics reflect mixing between partial melts of plume- and MORB-source mantle. The depleted mantle source component may reside within the shallow convecting mantle or within the base of the continental lithosphere.

6. Summary

The combination of geochemical and Sr–Nd isotopic data for the most primitive basic and ultrabasic magmas emplaced within the PDD rift with estimates for the amount of lithospheric extension (Kusznir et al., 1996a,b), strongly supports the involvement of a thermally and chemically anomalous mantle plume in the geodynamic evolution of the rift. Given the similar history of magmatism, rifting and domal basement uplift within all the Late Devonian rifts of the EEP (Fig. 1), it is suggested that a series of discrete mantle upwellings (plumes) may have impinged upon the base of the EEP lithosphere during mid-Frasnian–late Famennian times. Such plumes must have originated from at least the base of the upper mantle (670 km discontinuity). Lithospheric extension is likely to have been the consequence of far-field stresses related to plate-boundary forces. The thermal influence of the plumes in weakening the thick cratonic lithosphere must, however, have greatly facilitated rifting.

The Frasnian–Famennian boundary marks one of the five largest marine mass extinctions in the Phanerozoic (Wang et al., 1991; Claeys and Casier, 1994). There is some debate as to whether the extinction event was instantaneous, possibly associated with one or more bolide impacts (Claeys and Casier, 1994), or whether it took place over several million years. The voluminous Frasnian–Famennian magmatism of the EEP may have had a significant impact on global climate and must therefore be regarded as a potential causal factor in the mass extinction event.

Acknowledgements

This project forms part of a much larger project currently being undertaken by the Intraplate Tectonics and Basin Dynamics Working Group of EUROPROBE, which aims to further our understanding of the dynamics of sedimentary basin formation in Europe by means of integrated basin analysis and modelling. The EUROPROBE project involves close collaboration between M. Wilson (Leeds), R.A. Stephenson (Free University, Amsterdam), P.A. Ziegler (Basel, Switzerland) and the Academies of Science of the Ukraine (Kiev and Lvov) and Belarus (Minsk). This project was partially supported by NERC research grant GR9/859 to M. Wilson and by INTAS grant 93-3346. The assistance of Elizabeth Ann Dunworth, Jeff Rosenbaum and Alan Gray with geochemical and isotopic analyses is gratefully acknowledged.

References

Alekseev, A.S., Kononova, L.I. and Nikishin, A.M., 1996. The Devonian and Carboniferous of the Moscow Syneclise (Russian Platform): stratigraphy and sea-level changes. In: R.A. Stephenson, M. Wilson, H. de Boorder and V.I. Starostenko (Editors), EUROPROBE: Intraplate Tectonics and Basin Dynamics of the Eastern European Platform. Tectonophysics, 268: 149–168 (this volume).

de Boorder, H., van Beek, A.J.J., Dijkstra, A.H., Galetsky, L.S., Koldewe, G. and Panov, B.S., 1996. Crustal architecture of the Donets Basin: tectonic implications for diamond and mercury–antimony mineralization. In: R.A. Stephenson, M. Wilson, H. de Boorder and V.I. Starostenko (Editors), EUROPROBE: Intraplate Tectonics and Basin Dynamics of the Eastern European Platform. Tectonophysics, 268: 293–309 (this volume).

Chekunov, A.V., Gavrish, V.K., Kutas, R.I. and Ryabchun, L.I., 1992. Dnieper–Donets Paleo-rift. Tectonophysics, 208: 257–272.

Claeys, P. and Casier, J.-G., 1994. Microtektite-like impact glass associated with the Frasnian–Famennian boundary mass extinction. Earth Planet. Sci. Lett., 122: 303–315.

Fitton, G., Hardarson, B.S., Saunders, A.D. and Norry, M.J., 1996. The chemical distinction between depleted plume and N-MORB mantle sources. Abstract 1996 Goldschmidt Conference, J. Conf. Abstr., 1: 167.

Gerlach, D.C., Stormer, J.C. Jr. and Mueller, P.A., 1987. Isotopic geochemistry of Fernando de Noronha. Earth Planet. Sci. Lett., 85: 129–144

Gladkikh, V., 1971. Petrochemical and geochemical peculiarities of tholeiitic basalts of the Voronezh anteclise. Bulletin Moskovskoyo Obstchestova Ispytatelei Prirody, XLVI(2): 107–118 (in Russian).

Gon'shakova, V.I., Ruzhitskiy, V.O., Boychuk, M.D., Zaritsky, A.I. and Strekozov, N.F., 1967. Volcanic pipes and dykes of kimberlite rocks on the Russian Platform. Int. Geol. Rev., 11: 60–73.

Harland, W.B., Armstrong, R.L., Cox, A.V., Craig, L.E., Smith, A.G. and Smith, D.G., 1990. A Geological Time Scale 1989. Cambridge University Press, Cambridge, 236 pp.

Herzberg, C., 1995. Generation of plume magmas through time: an experimental perspective. Chem. Geol., 126: 1–16.

Kramm, U. and Kogarko, L.N., 1994. Nd and Sr isotope signatures of the Khibina and Lovozero agpaitic centres, Kola Alkaline Province, Russia. Lithos, 32: 225–242.

Kramm, U., Kogarko, L.N., Kononova, V.A. and Vartiainen, H., 1993. The Kola Alkaline Province of the CIS and Finland: precise Rb–Sr ages define 380–360 Ma age range for all magmatism. Lithos, 30: 33–44.

Kusznir, N.J., Stovba, S.M., Stephenson, R.A. and Poplavskii, K.N., 1996a. The formation of the northwestern Dnieper–Donets Basin: 2D forward and reverse syn-rift and post-rift modelling. In: R.A. Stephenson, M. Wilson, H. de Boorder and V.I. Starostenko (Editors), EUROPROBE: Intraplate Tectonics and Basin Dynamics of the Eastern European Platform. Tectonophysics, 268: 237–255 (this volume).

Kusznir, N.J., Kovkhuto, A. and Stephenson, R.A., 1996b. Syn-rift evolution of the Pripyat Trough: constraints from structural and stratigraphic modelling. In: R.A. Stephenson, M. Wilson, H. de Boorder and V.I. Starostenko (Editors), EUROPROBE: Intraplate Tectonics and Basin Dynamics of the Eastern European Platform. Tectonophysics, 268: 221–236 (this volume).

Le Bas, M.J., Le Maitre, R.W. and Woolley, A.R., 1992. The construction of the total alkali-silica chemical classification of volcanic rocks. Mineral. Petrol., 46: 1–22.

Mahotkin, I.L. and Juravlev, D.E., 1993. Sr and Nd isotopic data of diamond-bearing kimberlites and melilitites of the Archangelsk region. Dokl. Akad. Nauk, 332: 491–495.

McKenzie, D.P. and Bickle, M.J., 1988. The volume and composition of melt generated by extension of the lithosphere. J. Petrol., 29: 625–679.

Nikishin, A.M., Ziegler, P.A., Stephenson, R.A., Cloetingh, S., Furne, A.V., Fokin, P.A., Ershov, A.V., Bolotov, S.N., Korotaev, M.V., Alekseev, A.S., Gorbachev, V.I., Shipilov, E.V., Lankreijer, A., Bembinova, E.Yu. and Shalimov, I.V., 1996. Late Precambrian to Triassic history of the East European Craton: dynamics of sedimentary basin evolution. In: R.A. Stephenson, M. Wilson, H. de Boorder and V.I. Starostenko (Editors), EUROPROBE: Intraplate Tectonics and Basin Dynamics of the Eastern European Platform. Tectonophysics, 268: 23–63 (this volume).

Stephenson, R.A. and the EUROPROBE Intraplate Tectonics and Basin Dynamics Dnieper–Donets and Polish Trough working groups, 1993. Continental rift development in Precambrian and Phanerozoic Europe: EUROPROBE and the Dnieper–Donets Rift and Polish Trough basins. Sediment. Geol., 86: 159–175.

Sun, S.S. and McDonough, W.F., 1989. Chemical and isotopic systematics of oceanic basalts: implications for mantle composition and processes. In: A.D. Saunders and M.J. Norry (Editors), Magmatism in the Ocean Basins. Geol. Soc. London, Spec. Publ., 42: 313–345.

Ulmishek, G.F., Bogino, V.A., Keller, M.B. and Poznyakevich, Z.L., 1994. Structure, stratigraphy and petroleum geology of the Pripyat and Dnieper–Donets basins, Byelarus and Ukraine. In: S.M. Landon (Editor), Interior Rift Basins. Am. Assoc. Pet. Geol., Mem., 59: 125–156.

van Wees, J.D., Stephenson, R.A., Stovba, S.M. and Shymanovskyi, V.A., 1996. Tectonic variation in the Dniepr–Donets Basin from automated modelling of backstripped subsidence curves. In: R.A. Stephenson, M. Wilson, H. de Boorder and V.I. Starostenko (Editors), EUROPROBE: Intraplate Tectonics and Basin Dynamics of the Eastern European Platform. Tectonophysics, 268: 257–280 (this volume).

Wang, K., Orth, C.J., Attrep, M., Chatterton, B.D.E., Hou, H. and Geldsetzer, H.H.J., 1991. Geochemical evidence for a catastrophic biotic event at the Frasnian/Famennian boundary in south China. Geology, 19: 776–779.

White, R.S. and McKenzie, D.P., 1989. Magmatism in rift zones: the generation of volcanic continental margins and flood basalts. J. Geophys. Res., 94: 7685–7729.

Wilson, M., 1993a. Magmatism and the geodynamics of sedimentary basin formation. Sediment. Geol., 86: 5–29.

Wilson, M., 1993b. Geochemical signatures of continental and oceanic basalts: a key to mantle dynamics? J. Geol. Soc. London, 150: 977–990.

Winchester, J.A. and Floyd, P.A., 1977. Geochemical discrimination of different magma series and their differentiation products using immobile elements. Chem. Geol., 20: 325–343.

Zaitsev, A. and Bell, K., 1995. Sr and Nd isotope data of apatite, calcite and dolomite as indicators of source, and the relationships of phoscorites and carbonatites from the Kovdor massif, Kola peninsula, Russia. Contrib. Mineral. Petrol., 121: 324–335.

Ziegler, P.A., 1990. Collision related intra-plate deformations in Western and Central Europe. J. Geodyn., 11: 357–388.